J|A|C|S
ARTICLES
Published on Web 04/03/2004

Charge-Driven Flocculation of Poly(L-lysine)−Gold Nanoparticle Assemblies Leading to Hollow Microspheres

Vinit S. Murthy,[†] Jennifer N. Cha,[§] Galen D. Stucky,*[,§,||] and Michael S. Wong*[,†,‡]

Contribution from the Department of Chemical Engineering, MS-362, Department of Chemistry, Rice University, Houston Texas 77251-1892, and Department of Chemistry and Biochemistry and Materials Department, University of California, Santa Barbara California 93106

Received October 8, 2003; E-mail: mswong@rice.edu; stucky@chem.ucsb.edu

Abstract: An unusual aggregation phenomenon that involves positively charged poly(L-lysine) (PLL) and negatively charged gold nanoparticles (Au NPs) is reported. Discrete, submicrometer−sized spherical aggregates are found to form immediately upon combining a PLL solution with gold sol (diameter ≈ 14 nm). These PLL−Au NP assemblies grow in size with time, according to light scattering experiments, which indicates a dynamic flocculation process. Water-filled, silica hollow microspheres (outer diameter ≈ microns) are obtained upon the addition of negatively charged SiO_2 NPs (diameter ≈ 13 nm) to a suspension of the PLL−Au NP assemblies, around which the SiO_2 NPs form a shell. Structural analysis through confocal microscopy indicates the PLL (tagged with a fluorescent dye) is located in the interior of the hollow sphere, and mostly within the silica shell wall. The hollow spheres are theorized to form through flocculation, in which the charge-driven aggregation of Au NPs by PLL provides the critical first step in the two-step synthesis process ("flocculation assembly"). The SiO_2 shell can be removed and re-formed by decreasing and increasing the suspension pH about the point-of-zero charge of SiO_2, respectively.

Introduction

Recent years have seen the emergence of new synthesis routes to nanoparticle-based materials in which there is controlled, spatial ordering of the nanoparticle (NP) building blocks.[1−9] Such routes range from the cross-linking of NPs functionalized with molecules that participate in complementary binding (e.g., antibody−antigen,[10] DNA oligonucleotides,[11] streptavidin−biotin,[2] and diaminotriazine−thymine pairs[12]), to the organization of NPs into rings,[13] wires,[14,15] and superlattices[3,5,16,17] induced by solvent evaporation and by application of external fields.[18,19] Layer-by-layer assembly[20] has also been conceived to direct the formation of thin films, from oppositely charged nanoparticle and polymer layers that are sequentially adsorbed onto a substrate.[7,8,21] Through such bottom-up synthesis approaches, macroscopic NP-based structures that exhibit the optical, electronic, magnetic, or catalytic properties of the constituent NPs can be accessed.

There has been a revived interest in the synthesis of inorganic hollow microspheres (submicron and micron diameters) for potential use in therapeutic, storage, and catalytic applications.[8,22−25] Various chemical approaches to inorganic hollow sphere fabrication can be broadly classified into (1) sacrificial core method[8,26,27] and (2) interfacial synthesis,[28,29] in which the

[†] Department of Chemical Engineering, Rice University.
[‡] Department of Chemistry, Rice University.
[§] Department of Chemistry and Biochemistry, UCSB.
[||] Department of Materials, UCSB.

(1) Mirkin, C. A. *Inorg. Chem.* **2000**, *39*, 2258−2272.
(2) Niemeyer, C. M. *Angew. Chem., Int. Ed.* **2001**, *40*, 4128−4158.
(3) Collier, C. P.; Vossmeyer, T.; Heath, J. R. *Annu. Rev. Phys. Chem.* **1998**, *49*, 371−404.
(4) Shipway, A. N.; Katz, E.; Willner, I. *ChemPhysChem* **2000**, *1*, 18−52.
(5) Murray, C. B.; Kagan, C. R.; Bawendi, M. G. *Science* **1995**, *270*, 1335−1338.
(6) Liz-Marzan, L. M.; Norris, D. J.; Bawendi, M. G.; Betley, T.; Doyle, H.; Guyot-Sionnest, P.; Klimov, V. I.; Kotov, N. A.; Mulvaney, P.; Murray, C. B.; Schiffrin, D. J.; Shim, M.; Sun, S.; Wang, C. *MRS Bull.* **2001**, *26*, 981−984.
(7) Kotov, N. A. *MRS Bull.* **2001**, *26*, 992−997.
(8) Caruso, F.; Caruso, R. A.; Mohwald, H. *Science* **1998**, *282*, 1111−1114.
(9) Rogach, A. L.; Talapin, D. V.; E. V., S.; Kornowski, A.; Haase, M.; Weller, H. *Adv. Funct. Mater.* **2002**, *12*, 653−664.
(10) Shenton, W.; Davis, S. A.; Mann, S. *Adv. Mater.* **1999**, *11*, 449−452.
(11) Mucic, R. C.; Storhoff, J. J.; Mirkin, C. A.; Letsinger, R. L. *J. Am. Chem. Soc.* **1998**, *120*, 12 674−12 675.
(12) Boal, A. K.; Ilhan, F.; DeRouchey, J. E.; Thurn-Albrecht, T.; Russell, T. P.; Rotello, V. M. *Nature* **2000**, *404*, 746−748.
(13) Niemeyer, C. M.; Adler, M.; Gao, S.; Chi, L. F. *Angew. Chem., Int. Ed.* **2000**, *39*, 3055−3059.
(14) Lu, X. M.; Hanrath, T.; Johnston, K. P.; Korgel, B. A. *Nano Lett.* **2003**, *3*, 93−99.
(15) Korgel, B. A.; Fitzmaurice, D. *Adv. Mater.* **1998**, *10*, 661−665.
(16) Stowell, C.; Korgel, B. A. *Nano Lett.* **2001**, *1*, 595−600.
(17) Korgel, B. A.; Fullam, S.; Connolly, S.; Fitzmaurice, D. *J. Phys. Chem. B* **1998**, *102*, 8379−8388.
(18) Zeng, H.; Li, J.; Liu, J. P.; Wang, Z. L.; Sun, S. H. *Nature* **2002**, *420*, 395−398.
(19) Hermanson, K. D.; Lumsdon, S. O.; Williams, J. P.; Kaler, E. W.; Velev, O. D. *Science* **2001**, *294*, 1082−1086.
(20) Decher, G. *Science* **1997**, *277*, 1232−1237.
(21) Mamedov, A. A.; Kotov, N. A. *Langmuir* **2000**, *16*, 5530−5533.
(22) Duan, H. W.; Chen, D. Y.; Jiang, M.; Gan, W. J.; Li, S. J.; Wang, M.; Gong, J. *J. Am. Chem. Soc.* **2001**, *123*, 12 097−12 098.
(23) Fowler, C. E.; Khushalani, D.; Mann, S. *Chem. Commun.* **2001**, 2028−2029.
(24) van Bommel, K. J. C.; Jung, J. H.; Shinkai, S. *Adv. Mater.* **2001**, *13*, 1472−1476.
(25) Tsapis, N.; Bennett, D.; Jackson, B.; Weitz, D. A.; Edwards, D. A. *Proc. Natl. Acad. Sci. U.S.A.* **2002**, *99*, 12 001−12 005.
(26) Zhong, Z. Y.; Yin, Y. D.; Gates, B.; Xia, Y. N. *Adv. Mater.* **2000**, *12*, 206−209.
(27) Jiang, P.; Bertone, J. F.; Colvin, V. L. *Science* **2001**, *291*, 453−457.
(28) Kulak, A.; Davis, S. A.; Dujardin, E.; Mann, S. *Chem. Mater.* **2003**, *15*, 528−535.

10.1021/ja038953v CCC: $27.50

inorganic (or organic) shell can be considered to form around a solid or liquid core, respectively. These approaches can involve multiple steps and severe synthesis conditions in the formation of the shell and requires the removal of the sacrificial core after shell formation. By comparison, organic hollow spheres such as vesicles,[30−32] "knedels",[33,34] and "polymersomes"[35] are formed more easily from the self-assembly of amphiphilic molecules, but they are generally less stable and smaller in size.

Notable examples of hollow spheres composed of NPs have been reported recently. The layer-by-layer assembly of NPs into hollow microspheres was shown to be a versatile preparation route by Caruso and co-workers; the thin shell wall tended to deform and collapse after removal of the sacrificial latex core in many cases, though.[36−39] SiO_2 NPs were used to coat and stabilize micrometer-sized oil droplets by Binks and co-workers.[40] These structures are not stable after removal of the oil core because the shell wall is too thin and the NPs are not bound together. Cross-linking the particles was shown to be a successful method for a stable hollow sphere structure, in the case where latex microparticles were adsorbed around the water droplets and slightly sintered together (to form "colloidosomes").[29]

We recently reported on the synthesis of inorganic NP-based hollow spheres under ambient conditions and without a sacrificial template.[41] Silica/gold hollow spheres were generated through the formation of Au NP/poly(L-lysine-*b*-L-cysteine) copolymer aggregates and their subsequent encasement within a shell composed of SiO_2 NPs. It was proposed that Au NPs reacted with the poly(L-cysteine) block to form gold-thiolate covalent bonds and that negatively charged SiO_2 NPs interacted electrostatically with the positively charged poly(L-lysine). We found that the synthesis chemistry permitted the formation of silica hollow spheres containing silver NPs[41] and CdSe/CdS quantum dots.[42] For the latter material, it was suggested that electrostatic interactions contributed significantly to the formation of quantum dot/poly(L-lysine-*b*-L-cysteine) copolymer aggregates. We subsequently found that poly(L-lysine) formed hollow spheres with quantum dots and SiO_2 NPs without the poly(L-cysteine) block; we hypothesized the formation of quantum dots/PLL vesicle structures as the intermediate precursor to the hollow spheres.[43] In this work, we provide new results indicating that the formation of NP−based hollow spheres may be described as a type of flocculation of NPs by charged polymers.

The phenomenon of particle flocculation as a route to functional materials has not been emphasized thus far. Flocculation is generally a random process in which polyelectrolytes bind nonselectively and nondirectionally to oppositely charged particles. Charge neutralization and formation of interparticle polymer bridges are identified as the two key mechanistic steps involved in flocculation,[44] but the lack of spatial and directional control of the binding and bridging results in randomly structured, fractal-like particle/polymer precipitate.[45−47] Flocculation of (submicron to micron sized, 100's−1000's nm) particles has been studied over the last fifty years and has seen applications in refining mineral ores, paper manufacture, water remediation, food industry, and pharmaceuticals, for example. Extensive experimental and theoretical work continues today to understand better the kinetics of flocculation and the internal structure of the flocculent material (e.g., floc size distribution and interparticle distances), particularly for NPs (<100 nm).[48−50] A better understanding and control of the flocculation process would ultimately be needed to construct NP-based flocculated materials of controlled structure.

In this work, we report the formation of spherical, submicron flocs of Au NPs and poly(L-lysine) (PLL), and demonstrate that the gold−thiolate bonds proposed for the poly(L-lysine-*b*-L-cysteine) copolymer system is not required in the synthesis of hollow microspheres. We investigate the unusual aggregation properties of Au NPs with PLL through confocal microscopy and dynamic light scattering, and discuss their effect on the hollow sphere structure resulting from shell formation.

Experimental Section

Materials. Poly(L-lysine) (PLL) was procured as a hydrogen bromide salt (Sigma−Aldrich) and was used as-received. PLL1 and PLL2 are polymers with two different lengths, and PLL3 is a longer polymer covalently conjugated to fluorescein isothiocyanate (FITC) through the ϵ-amino group (Table 1). Starting polymer solutions (2 mg/mL) were prepared with 18.2 MΩ deionized water and kept refrigerated when not in use (pH ≈ 6.2).

Table 1. Various Poly-L-lysines Used for Experiments along with Their Size and Polydispersity Information

poly-L-lysine	molecular weight, kD[a]	dispersity index, M_w/M_n[a]	contour length, nm	hydrodynamic diameter, nm[b]
PLL1	27.4	1.3	∼ 49	∼ 30
PLL2	57.9	1.15	∼ 104	∼ 45
PLL3[c]	68.6	NA	∼ 123	NA

[a] Data provided by the supplier. [b] Measured by dynamic light scattering. [c] FITC content: 0.006 mol/(mol lysine unit), reported by supplier.

Au NPs were synthesized through the citrate reduction method.[51,52] The NPs were 14 ± 2 nm in diameter as characterized by transmission

(29) Dinsmore, A. D.; Hsu, M. F.; Nikolaides, M. G.; Marquez, M.; Bausch, A. R.; Weitz, D. A. *Science* **2002**, *298*, 1006−1009.
(30) Checot, F.; Lecommandoux, S.; Gnanou, Y.; Klok, H. A. *Angew. Chem., Int. Ed.* **2002**, *41*, 1339−1343.
(31) Walker, S. A.; Kennedy, M. T.; Zasadzinski, J. A. *Nature* **1997**, *387*, 61−64.
(32) Antonietti, M.; Forster, S. *Adv. Mater.* **2003**, *15*, 1323−1333.
(33) Huang, H. Y.; Remsen, E. E.; Kowalewski, T.; Wooley, K. L. *J. Am. Chem. Soc.* **1999**, *121*, 3805−3806.
(34) Thurmond, K. B.; Kowalewski, T.; Wooley, K. L. *J. Am. Chem. Soc.* **1996**, *118*, 7239−7240.
(35) Discher, B. M.; Won, Y. Y.; Ege, D. S.; Lee, J. C. M.; Bates, F. S.; Discher, D. E.; Hammer, D. A. *Science* **1999**, *284*, 1143−1146.
(36) Khopade, A. J.; Caruso, F. *Nano Lett.* **2002**, *2*, 415−418.
(37) Schuler, C.; Caruso, F. *Biomacromolecules* **2001**, *2*, 921−926.
(38) Park, M. K.; Xia, C. J.; Advincula, R. C.; Schutz, P.; Caruso, F. *Langmuir* **2001**, *17*, 7670−7674.
(39) Caruso, F.; Yang, W. J.; Trau, D.; Renneberg, R. *Langmuir* **2000**, *16*, 8932−8936.
(40) Binks, B. P.; Lumsdon, S. O. *Phys. Chem. Chem. Phys.* **1999**, *1*, 3007−3016.
(41) Wong, M. S.; Cha, J. N.; Choi, K. S.; Deming, T. J.; Stucky, G. D. *Nano Lett.* **2002**, *2*, 583−587.
(42) Cha, J. N.; Bartl, M. H.; Wong, M. S.; Popitsch, A.; Deming, T. J.; Stucky, G. D. *Nano Lett.* **2003**, *3*, 907−911.
(43) Cha, J. N.; Birkedal, H.; Euliss, L. E.; Bartl, M. H.; Wong, M. S.; Deming, T. J.; Stucky, G. D. *J. Am. Chem. Soc.* **2003**, *125*, 8285−8289.
(44) Dickinson, E.; Eriksson, L. *Adv. Colloid Interface Sci.* **1991**, *34*, 1−29.
(45) Biggs, S.; Habgood, M.; Jameson, G. J.; Yan, Y. D. *Chem. Eng. J.* **2000**, *80*, 13−22.
(46) Glover, S. M.; Yan, Y. D.; Jameson, G. J.; Biggs, S. *Chem. Eng. J.* **2000**, *80*, 3−12.
(47) Thomas, D. N.; Judd, S. J.; Fawcett, N. *Water Res.* **1999**, *33*, 1579−1592.
(48) Berlin, A. A.; Solomentseva, I. M.; Kislenko, V. N. *J. Colloid Interface Sci.* **1997**, *191*, 273−276.
(49) Larsson, A.; Walldal, C.; Wall, S. *Colloid Surf. A-Physicochem. Eng. Asp.* **1999**, *159*, 65−76.
(50) Wong, K.; Cabane, B.; Somasundaran, P. *Colloids Surf.* **1988**, *30*, 355−360.
(51) *Immuno-Gold Labeling in Cell Biology*; CRC Press: Boca Raton, Florida, 1989.

Table 2. Nanoparticles Used for Experiments

nanoparticle	hydrodynamic diameter, nm	ζ potential, mV	concentration, particles/mL
Au NP	14 ± 2	−45	2.67×10^{12}
SiO_2 NP	13 ± 3	−16	1.14×10^{17}

electron microscopy and dynamic light scattering. The number concentration of the stock colloidal sol (pH ≈ 7.0) was estimated from the optical density at the plasmon resonance frequency (520 nm) using an extinction coefficient of 2.4×10^8 $M^{-1}cm^{-1}$; an optical density value of 1.064 gave a concentration of 4.43×10^{-9} M (2.67×10^{12} NP/mL).[1] SiO_2 NPs (Snowtex O, Nissan Chemicals) were supplied as a colloidal sol (20.4 wt % solids, pH 3.4); the number concentration was calculated to be 1.14×10^{17} NP/mL. These NPs measured 13 ± 3 nm in diameter as characterized by dynamic light scattering. The zeta (ζ) potentials of Au and SiO_2 NPs were calculated from their electrophoretic mobility (measured in their native solution) using Henry's equation,[53] respectively (Table 2). The value for the Au NP zeta potential is underestimated,[54] but does not affect the conclusions of this paper.

Synthesis. The synthesis of SiO_2/Au NP-based hollow spheres is accomplished in two steps, similar to that described by Wong et al.[41] 125 μL of the Au colloidal sol was micropipetted into a 1.5 mL microcentrifuge test tube that contained 21 μL of a PLL solution (2 mg/mL). The synthesis mixture was agitated at low speed ("4" speed on a 1−10 scale) for 10 s using a vortex mixer (Fisher Scientific), to provide thorough and rapid homogenization and mixing of the Au NP/PLL suspension. To this suspension, 125 μL of SiO_2 sol was added immediately and vigorously vortex-mixed ("8" speed) for 20 s, resulting in water-containing microspheres. The final pH of the synthesis mixture was measured to be 4.9.

For the hollow sphere size control experiments, the floc suspension was left to stand for 3 min, 20 min, or 2 h before the SiO_2 sol was added.

For studying the pH effect on the hollow sphere structure, the as-prepared sphere suspension (pH ≈ 4.9) was acidified by adding 40 μL of 1 N HCl and vortex-mixed at "8" speed for 10 s (final pH ≈ 0.5). The cloudy suspension turned clear. It was then combined with 60 μL of 1 N NaOH and vortex-mixed at "8" speed for 10 s (final pH ≈ 10), with the suspension turning cloudy again.

Characterization. Confocal Laser Scanning Microscopy. Confocal images were captured with Carl Zeiss LSM 410 inverted confocal microscope equipped with a 100× oil immersion objective (NA = 1.4). The laser excitation wavelength of 488 nm was chosen for FITC (λ_{Ex} = 494.5 nm, λ_{Em} = 519 nm). Samples were mounted on conventional glass slides and sealed under a cover slip to prevent drying. All samples were prepared 1−2 h prior to imaging.

Image Processing. A freely available NIH image processing software called "*ImageJ*"[55] was used for calculating the line intensity profile across the sphere. Also, the size distribution of spheres (>300 spheres were analyzed for each sample) from confocal microscopy images was measured with this software. Adobe Photoshop V6.0 was used to enhance the images; it was ensured that there was no loss of information or incorporation of any image processing artifacts.

Dynamic Light Scattering. Size distribution and zeta potential analysis were carried out with Brookhaven ZetaPALS dynamic light scattering (DLS) equipment with BI-9000AT digital autocorrelator at 656 nm wavelength. All studies were done at a 90° scattering angle and temperature controlled at 25 °C; standard 50 μL cuvettes were used for size distribution analysis. Two types of size analysis studies were performed in this work. Time−averaged particle size distributions were collected over an analysis time of at least 15 min using the software package "*9KDLSW.*" For studying the evolution of Au NP/PLL flocs with time, time dependent size measurements were taken of Au NP/PLL floc suspensions immediately after vortex mixing, at 1−minute intervals using the software package "9KPSDW". Measurements of Au NP/PLL flocs started three minutes after the 10−second vortex mixing (the three-minute time gap was due to transferring the suspension from the synthesis vial to the DLS cuvette and parameter setup).

Zeta Potential Analysis. Zeta potentials were calculated using phase analysis light scattering (PALS), a variation of electrophoretic dynamic light scattering (DLS),[56] from electrophoretic mobility measurements using Henry's equation[53] (i.e., $0.1 \leq \kappa a \leq 100$, where κ is the Debye-Hückel parameter and a is the particle radius). A dip-in (Uzgiris type) electrode system[57] with 4 mL polystyrene cuvettes was used.

Fluorescence Spectroscopy. Fluorescence measurements were taken with Jobin-Yvon Horiba Fluoromax 3 spectrophotometer. Standard quartz cells with a path length of 1 cm were used. Solutions were constantly stirred during analysis with a magnetic Teflon bar; it was verified that the stirring did not contribute to any interference in the fluorescence spectrum.

UV−Vis Spectroscopy. Absorption spectroscopy was carried out in Shimadzu 2401-PC UV−vis spectrophotometer to characterize the Au NP. Standard quartz cuvettes with a path length of 1 cm were used.

Coulter Counter. Sphere size distribution was measured with a Beckman Coulter counter having an orifice diameter of 50 μm. The lower limit for measuring sizes for this equipment was 1 μm. 10 μL of a hollow sphere suspension (as synthesized) was diluted in 10 mL of aqueous Isotone solution (composition: 7.93 g/L NaCl, 0.38 g/L Na_2EDTA, 0.40 g/L KCl, 0.19 g/L H_2NaPO_4, 1.95 g/L HNa_2PO_4, 0.30 g/L NaF; Beckman Coulter).

Scanning Electron Microscopy. Scanning electron microscopy (SEM) was carried out in JEOL 6500 field emission microscope equipped with in-lens thermal field emission electron gun. Secondary electron image (SEI) was taken at 15 kV electron beam with a working distance of 10.0 mm. The microsphere suspension was aged for 2 days, washed with Isotone solution, and suspended in 2-propanol before being loaded and air-dried onto carbon tape for imaging.

Transmission Electron Microscopy. Transmission electron microscopy was performed on JEOL 2010 FasTEM system at 100 kV electron beam accelerating voltage. Microspheres aged for 2 days were washed with Isotone solution, suspended in 2-propanol, and loaded on a 200 mesh copper grid.

Results and Discussions

We first describe the formation of SiO_2/Au NP-based hollow microspheres using dye-tagged PLL, and then discuss the formation of the Au NP/polymer flocs and its importance to microsphere formation.

Hollow Microsphere Formation. Figure 1a shows the confocal image of a homogeneous aqueous solution of PLL3, in which no visible aggregates in the solution were observed. The conformation of PLL ($pK_a \approx 11.1$) in aqueous solution depends on the degree of protonation of the ϵ-amino group of the side chain. At neutral pH, the polymer would be in an extended, random coil conformation due to complete protonation. The addition of the negatively charged Au NPs to PLL3 clearly led to the formation of Au NP/PLL3 flocs, observed as discrete fluorescent spots at different focal planes in the z-direction (Figure 1b). Most of the flocs appeared larger than

(52) Frens, G. *Nat. Phys. Sci.* **1973**, *241*, 20−22.
(53) Rajagopalan, R.; Hiemenz, P. C. *Principles of Colloid and Surface Chemistry*; 3rd ed.; Marcel Dekker: New York, 1997.
(54) Kimura, K.; Takashima, S.; Ohshima, H. *J. Phys. Chem. B* **2002**, *106*, 7260−7266.
(55) http://rsb.info.nih.gov/ij/.
(56) McNeil-Watson, F.; Tscharnuter, W.; Miller, J. *Colloid Surf. A-Physicochem. Eng. Asp.* **1998**, *140*, 53−57.
(57) "Instruction Manual for BI-Zeta Potential Option," Brookhaven Instrument Corporation, 2000.

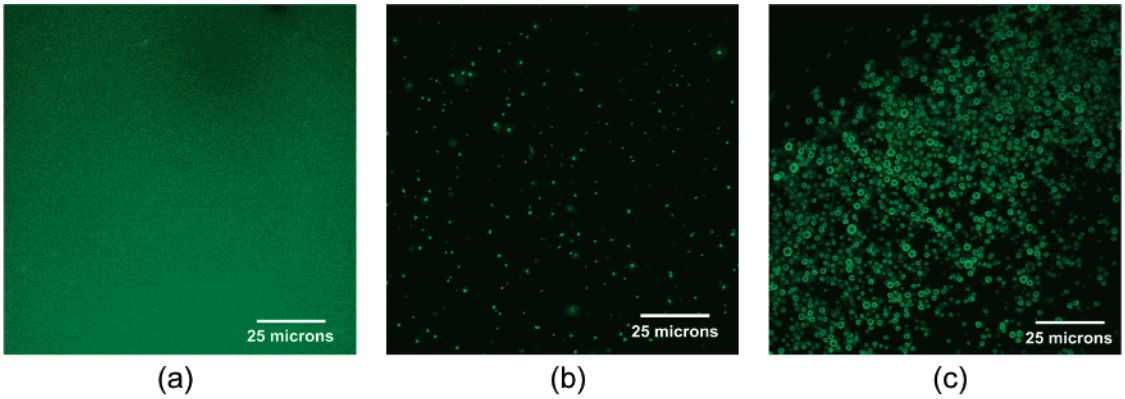

Figure 1. Confocal microscopy images showing the step-by-step formation of microspheres using PLL, Au NP, and SiO_2 NP. (a) PLL3 (conjugated to FITC dye) in solution, (b) globular flocs formed from Au NP/PLL3, and (c) microspheres formed after addition of SiO_2 NP to Au NP/PLL3 flocs.

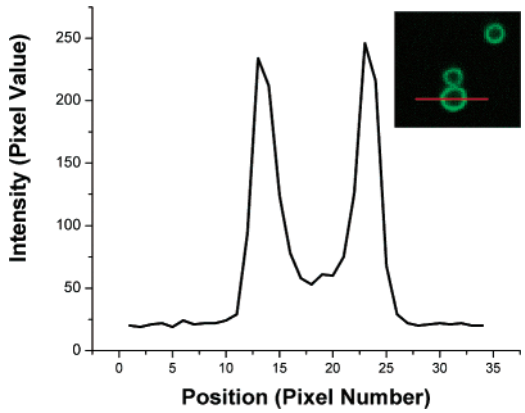

Figure 2. Line intensity profile across a microsphere showing the core-shell structure. Note that the fluorescence intensity is nonzero in the core and in the background.

their actual sizes in solution, likely due to their spreading on contact with glass (cover slip and glass slide). The larger flocs were spherical in shape and uniformly fluorescent within each floc.

SiO_2 NP addition to the Au NP/PLL3 suspension resulted instantaneously in hollow spheres, in which the SiO_2 NPs adsorbed around the Au NP/PLL3 flocs. The observed fluorescent ring structure (Figure 1c) indicated the presence of PLL3 within the SiO_2 shell wall. The core region of the hollow spheres exhibited weak but nonzero fluorescence, which was verified through line intensity profile analysis (Figure 2). The hollow sphere interior contained PLL3, but apparently at a lower concentration than that in the shell wall. PLL1 and PLL2 gave rise to hollow microspheres also (see the Supporting Information).

When the spheres were air-dried overnight after aging for 2 days in suspension, and subjected to reduced pressure for 10 min, the microspheres decreased roughly by 50% in diameter (Figure 3); the size reduction was verified to result from drying and not from the low pressure.

The dried spheres exhibited fluorescence from the shell wall and, curiously, from the core interior also (Figure 3b). Confocal microscopy eliminates fluorescence contributions from sample features not in the focal plane, and so the observed fluorescence from the microsphere interior indicated the presence of the FITC-tagged PLL suspended within the center of the spheres. TEM images of PLL3/Au NP/SiO_2 NP hollow spheres confirmed the presence of the hollow (Figure 4). The TEM image also provides evidence that hollow spheres as small as ~700 nm in diameter can be prepared.

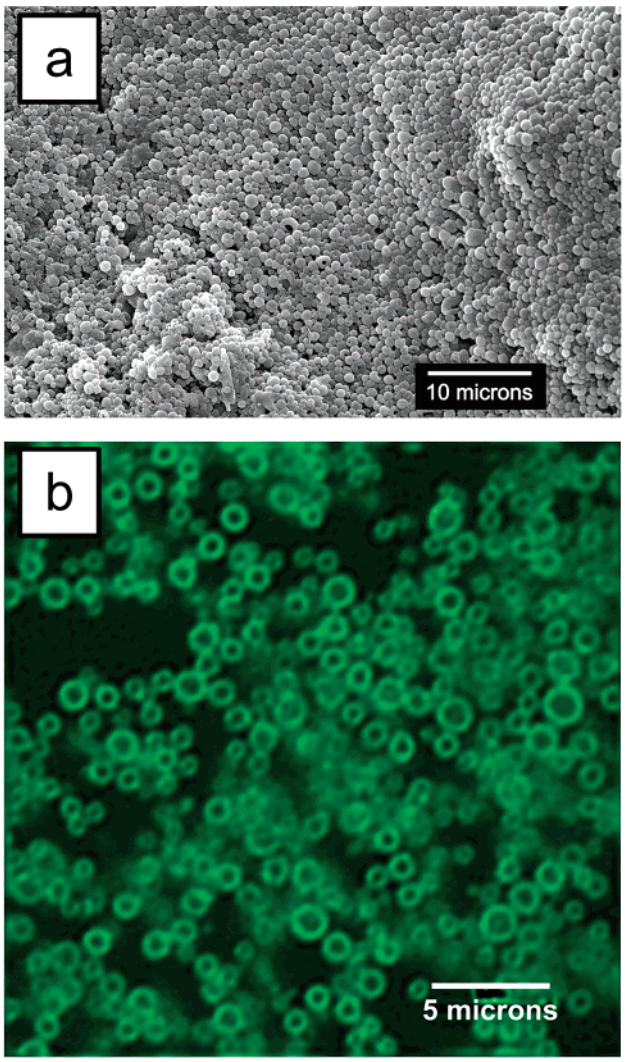

Figure 3. (a) Scanning electron microscopy image and (b) confocal microscopy image of microspheres (made from PLL3) after they have been dried and subjected to a vacuum of 5×10^{-5} torr at room temperature. Autoquant deblurring software was used to process the raw image in Figure 3b.

Au NP/PLL Floc Formation. Charge-driven flocculation occurs when a colloidal sol is destabilized by the adsorption of oppositely charged polyelectrolytes, which neutralizes the particle surface charge and leads to interparticle polymer

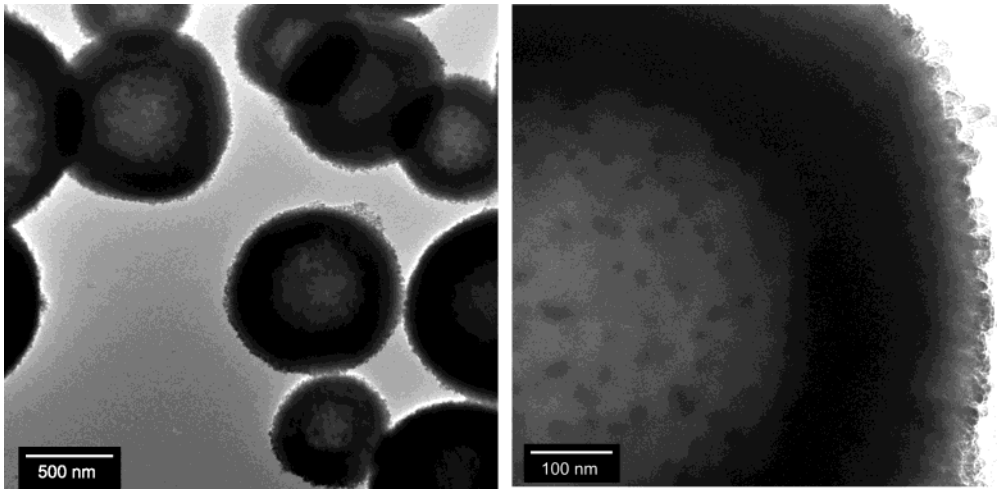

Figure 4. TEM images of hollow spheres made from PLL-FITC/Au NP/SiO_2 NP. The spheres were aged for 6 days before imaging.

bridging.[58−61] The initial flocculation period for Au NPs in the presence of salts under rapid coagulation conditions (von Smoluchowski kinetics) is known to be very short, with a characteristic aggregation time of about 60 milliseconds and a coagulation rate constant of 12.2×10^{-18} m^3/s (at 298 K).[61] We expect the initial stages of Au NP/PLL flocculation to follow rapid coagulation kinetics also, in which PLL binds to several NPs (to form a "multiplet").[62,63] Floc growth after initial formation is generally not well understood still, as nonequilibrium conditions combined with the simultaneous fast dynamics of polymer adsorption, floc restructuring, and interparticle collisions under turbulent mixing conditions complicate the study of flocculation.[64] Still, some conclusions can be made for the Au NP/PLL floc system.

Light scattering experiments were performed on the floc suspension to study the Au NP/PLL floc size as a function of aging time. Larger Au NP/PLL flocs were found with longer aging times and with larger molecular weights (Figure 5). The floc sizes ranged from a hydrodynamic diameter of 440 nm (at 3 min with the shortest PLL chain, PLL1) to 1.1 μm (at 21 min with the longest PLL chain, PLL3), much larger than the measured hydrodynamic diameters of the polymer and Au NPs (Tables 1 and 2). The hydrodynamic diameter was found to increase monotonically with time for all three PLL chain lengths, with fluctuations appearing after 15 min. Such time-growth behavior of polymer-colloidal particle flocs has been observed before.[45,65,66]

The shape of the floc growth curves can provide insights into the aggregation process of the polymer and the Au NPs. Assuming irreversible aggregation of PLL and NPs upon contact, a linear increase in floc diameter with time indicates the flocculation is reaction-limited, in which the adsorption of

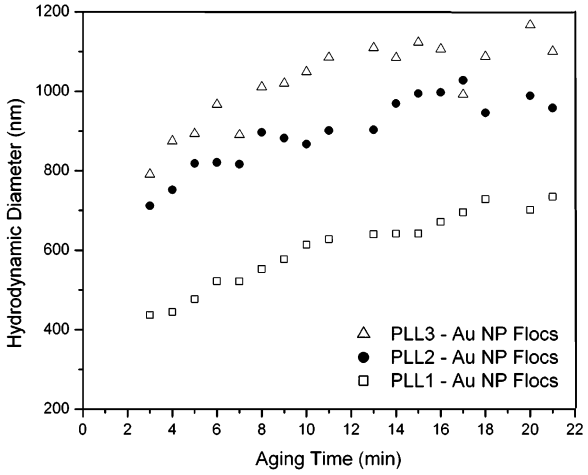

Figure 5. DLS time measurements of Au NP/PLL floc suspensions prepared with different PLL chain lengths. The error bar at each data point was ± 20 nm.

polymer and/or NP onto the floc occurs at a slower rate than their bulk diffusion to the floc outer surface. A sub-linear, square-root dependence of diameter to time, on the other hand, indicates a diffusion-limited flocculation process (in which adsorption occurs at a faster rate than diffusion). In our case, Au NP/PLL floc growth appears better described as a diffusion-limited process than a reaction-limited one.

Additional mechanisms may be involved during floc growth and cannot be ruled out yet: (1) the internal restructuring of smaller flocs of higher density into larger flocs of lower density (at constant floc population) to minimize the ensemble entropy;[62] (2) coalescence of smaller flocs into larger flocs (with decreasing floc population); (3) Ostwald ripening, in which the larger flocs grow at the expense of smaller flocs (with decreasing floc population); and (4) a combination of some or all of these processes.

Spectroscopy measurements of the Au NP/PLL3 floc suspensions before and after vortex mixing and aging for 5 min indicated ~90% of the polymer was incorporated into the floc structures. This percentage did not change when the flocs were aged for 15 h, suggesting that floc growth occurs through some process other than the incorporation of free polymer. Additional findings have also indicated that floc formation is sensitive to other factors, such as ionic strength and temperature of the

(58) Spalla, O. *Curr. Opin. Colloid Interface Sci.* **2002**, *7*, 179−185.
(59) Finch, C. A., Ed. *Industrial Water Soluble Polymers*; Royal Society of Chemistry: Cambridge, U.K., 1996.
(60) Sonntag, H.; Strenge, K. *Coagulation Kinetics and Structure Formation*; Plenum Press: New York, 1987.
(61) Dobias, B., Ed. *Coagulation and Flocculation*; Marcel Dekker: New York, 1993.
(62) Nowicki, W. *Colloid Surf. A-Physicochem. Eng. Asp.* **2001**, *194*, 159−173.
(63) Spalla, O.; Cabane, B. *Colloid Polym. Sci.* **1993**, *271*, 357−371.
(64) Adachi, Y.; Matsumoto, T.; Stuart, M. A. C. *Colloid Surf. A-Physicochem. Eng. Asp.* **2002**, *207*, 253−261.
(65) Ovenden, C.; Xiao, H. N. *Colloid Surf. A-Physicochem. Eng. Asp.* **2002**, *197*, 225−234.
(66) Spicer, P. T.; Pratsinis, S. E. *Water Res.* **1996**, *30*, 1049−1056.

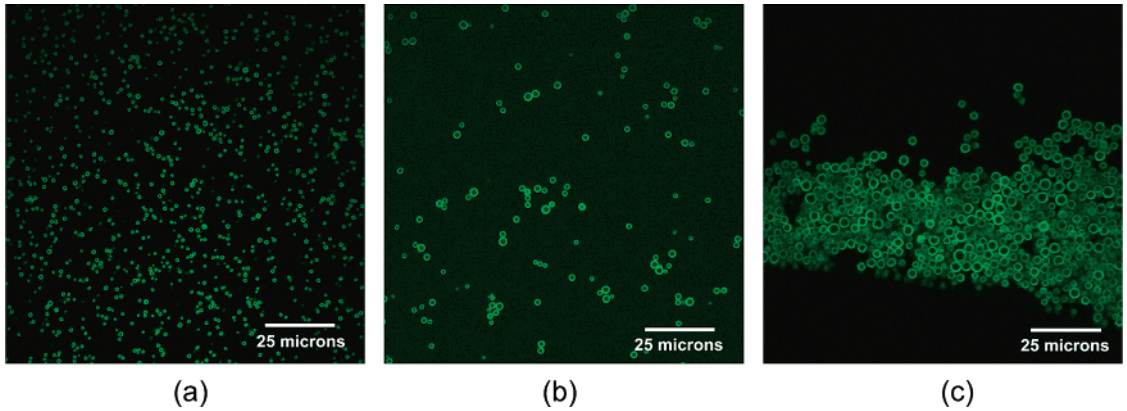

Figure 6. Confocal images of hollow microspheres prepared for Au NP/PLL3 floc suspensions aged from (a) 3 min, (b) 20 min, and (c) 2 h.

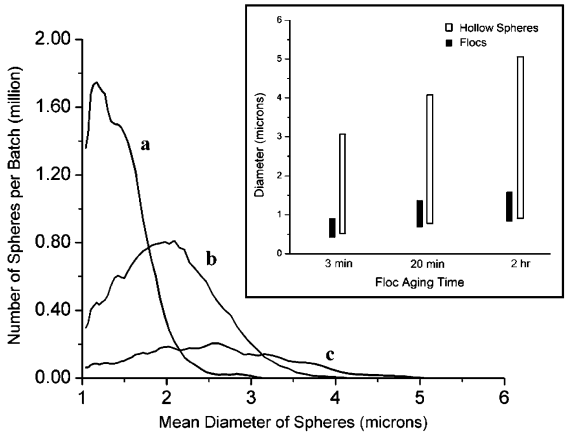

Figure 7. Coulter counter analysis of hollow microspheres prepared from Au NP/PLL3 floc suspensions aged for (a) 3 min, (b) 20 min, and (c) 2 h. The lower limit of detection was 1.04 μm. Inset: comparison of size distributions of the Au NP/PLL3 flocs (from DLS) and resultant hollow microspheres (from Coulter counter and confocal image analysis).

suspending aqueous medium. Comprehensive studies to understand better the Au NP/PLL flocculation process, particularly at short aging times, is currently underway.

Sphere Size Control. The strong dependence of aging time on Au NP/PLL floc size suggested a method to control the size of the silica hollow spheres. This hypothesis was tested by synthesizing spheres from Au NP/PLL3 floc suspensions aged for different times (i.e., 3 min, 20 min, and 2 h), and indeed, a distinct size difference was observed among the resultant hollow spheres (Figure 6).

Coulter counter measurements revealed that, with increased floc aging time, (1) the average sphere size increased, (2) the size distribution broadened, and (3) the sphere population decreased (Figure 7). The size and size distribution of the hollow microspheres are several times larger than those of the corresponding Au NP/PLL3 flocs, which could point to a rapid floc−floc aggregation during SiO_2 shell formation which leads to the severalfold larger hollow spheres (Figure 7, inset). From Coulter counter and confocal image analyses, the hollow sphere yields were estimated at 25, 14, and 3.5 million spheres per batch, prepared from floc suspensions aged for 3 min, 20 min, and 2 h, respectively.

Interestingly, the fluorescence emanating from the hollow sphere core appeared to vary with sphere diameter, based on intensity profile analysis of different sized spheres within a single confocal image frame (Figure 6b,c). The hollow spheres exhibited little to no fluorescence from the interior when the diameter exceeded ~4 μm. The Au NP/PLL floc core may be structurally unstable inside the larger spheres even when suspended in a water medium, resulting in adsorption of PLL chains and Au NPs onto the inner wall of the sphere.

Proposed Formation Mechanism of Hollow Spheres. Floc formation is the key step in microsphere synthesis, which was confirmed by changing the reaction order of the precursors. Combining SiO_2 NPs and PLL3 led to sheetlike aggregates, which did not lead to hollow spheres after Au NP addition (Figure 8b). Combining PLL3 with a mixed SiO_2 and Au NP sol led to sheetlike aggregates also (Figure 8c), indicating the importance of the Au NP/PLL3 floc to the formation of hollow spheres.

A formation mechanism that accounts for the dynamic growth of the Au NP/PLL floc intermediate is proposed (Scheme 1). In the two-step formation process, the PLL molecules bind electrostatically to negatively charged Au NPs. The PLL chain can bind to multiple NPs and NPs can serve as docking sites for multiple PLL chain adsorption, thereby leading to bridging flocculation.[44,45,67] Poly(allylamine) was also observed to form flocs with Au NPs, which leads to the contention that Au NP/polymer floc aggregates can be induced by cationic polyelectrolytes. The floc assemblies continue to grow with time after combining and mixing the two precursors together, in a dynamic process that can be exploited to form larger hollow spheres. The floc acquires a positive charge due to an excess of polymer concentration over the Au NPs (confirmed through ζ potential measurements). On the addition of silica sol, the negatively charged SiO_2 NPs adsorb onto the floc surface and initiates the formation of the shell structure. The SiO_2 shell wall is thick and contains multiple layers of SiO_2 NPs (Figure 4), and PLL chains are incorporated within the shell to bind the SiO_2 NPs together (Figure 1c); how the PLL and the NPs combine to form the thick shell is still under investigation. The final, as-synthesized hollow spheres contain the Au NP/PLL floc and water in the center, of which the relative amounts depend on the sphere size.

Reversible Assembly of Hollow Spheres. An interesting feature of the as-prepared hollow spheres is their ability to disassemble and re-assemble in response to pH variations in the suspension medium. It was conjectured that, if electrostatics were primarily the driving force in the shell formation, the shell could be broken apart by "turning" off or reversing the SiO_2

(67) Akinchina, A.; Linse, P. *Macromolecules* **2002**, *35*, 5183−5193.

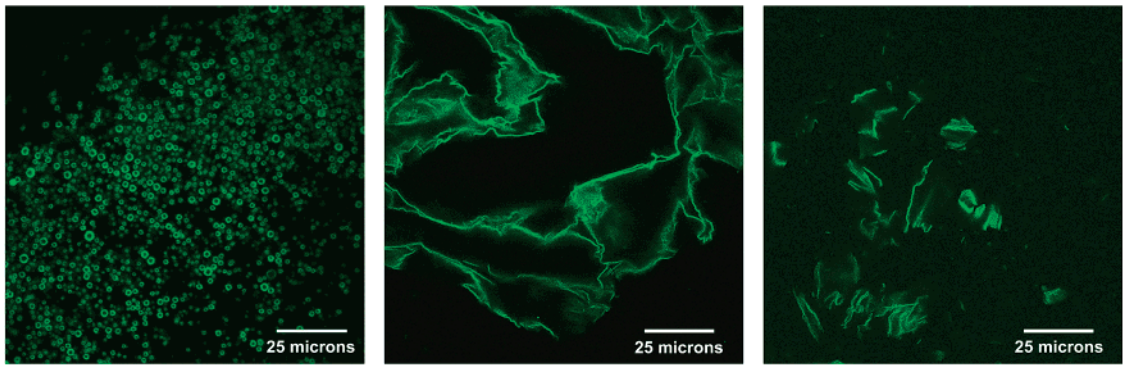

Figure 8. Confocal images of resultant suspensions (a) after SiO_2 NPs were added to Au NP/PLL3 flocs, (b) after Au NPs were added to SiO_2 NP/PLL3, and (c) after PLL3 was added to a combined Au NP/SiO_2 NP sol.

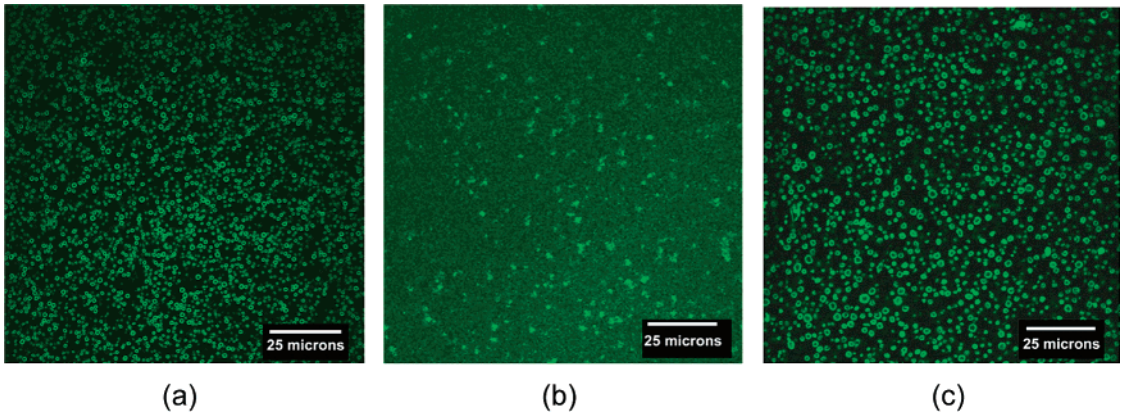

Figure 9. Images from confocal microscopy showing the structural reversibility of microspheres using a pH trigger. (a) As prepared hollow sphere suspension (pH ≈ 4.9), (b) acidification of suspension (final pH ≈ 0.5) causes the spheres to break due to re-dispersion of SiO_2 NP wall, and (c) addition of base to the acidified suspension re-assembles the microspheres (final pH ≈ 10.0).

Scheme 1. Proposed Flocculation-Based Self-Assembly of Organic−Inorganic Hollow Spheres from PLL, Au NPs, and SiO_2 NPs.

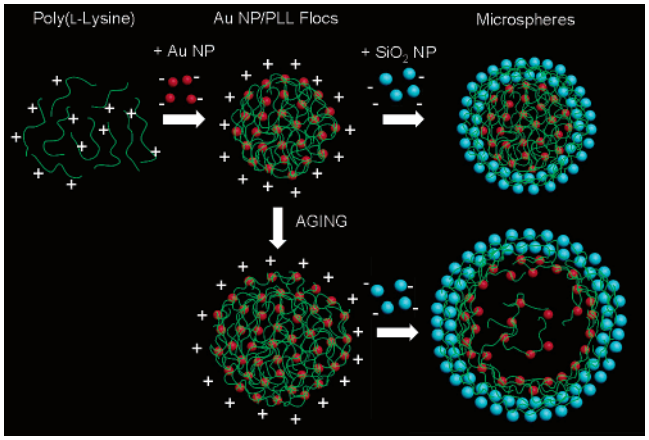

surface charge. The point-of-zero charge of SiO_2 is ∼2, and so the net surface charge would be negative at pH's above this value (e.g., the final synthesis pH of 4.9). When the original hollow sphere suspension (Figure 9a) was acidified and subsequently imaged through confocal microscopy, only bright spots and a fluorescent background were observed (Figure 9b). Hollow spheres were concluded to be broken down, releasing Au NP/PLL3 flocs and free PLL3 into solution. The pH of the suspension was then increased to ∼10, at which hollow spheres were again detected, thus indicating re-assembly (Figure 9c). A higher pH than the original synthesis pH of 4.9 was required to counteract the effect of increased ionic strength of the suspension (due to the additions of acid and base).

Conclusions

In this paper, we have demonstrated that PLL and Au NPs form (sub)micron-sized flocculated aggregates that are critical to the formation of organic−inorganic NP-based hollow spheres. The formation of the spherical floc structures is consistent with charge-driven flocculation, in which polyelectrolyte molecules can adsorb onto several oppositely charged colloidal particles, and the particles can bind to more than one polyelectrolyte chain. The Au NP/PLL flocs act as a template around which SiO_2 NPs and PLL molecules adsorb to form a stable silica shell. The sizes of the hollow spheres can be roughly adjusted by the size of the Au NP/PLL floc (determined by aging time of the floc suspension). The floc structure within the sphere appears to span the volume of the hollow sphere interior, except if the spheres are larger than ∼4 μm. The formation of Au NP/polymer flocs may be generalized (from PLL and poly(allylamine)) to any cationic polyelectrolyte.

The two-step formation of these Au and SiO_2 NP-based hollow spheres can be considered an NP self-assembly process induced by the presence of polyelectrolytes, in which the hollow spheres are rapidly generated at room temperature, near neutral pHs, in water, without the need of a solid template, and with minimal human intervention. These attributes of the flocculation

based self-assembly (or "flocculation assembly") of NPs into hollow microspheres provide new opportunities in encapsulation and release not available to other types of hollow sphere materials. It is intriguing that such a hierarchically structured material can be built from NPs, even though the electrostatic interactions between the charged NP surface and polymer molecule are nonspecific and nondirectional. Clearly, some concepts of flocculation help to explain the formation of these hollow spheres, particularly the first step of Au NP/polymer floc formation.

Acknowledgment. We thank Dr. K. Beckingham (Department of Biochemistry, Rice University) for use of the confocal microscope and Dr. M. Pasquali (Department of Chemical Engineering, Rice University) for use of the fluorescence microscope. We acknowledge Mr. A. Yee for assistance with the Coulter counter measurements, Mr. R. Duggal for assistance with the fluorescence microscope, Ms. E. Whitsitt for the SEM data, Mr. K. Mathur for assistance with image analysis, Mr. W. Knowles for the TEM image, Ms. J. Yu for helpful discussions, and Mr. R. A. Horch for assistance on the graphics. We gratefully acknowledge the financial support of Rice University and the National Science Foundation (NSF EEC-0118007) through the Center for Biological and Environmental Nanotechnology (CBEN), and NSF DMR 444-012-21219 (G.D.S.).

Supporting Information Available: SEM images of hollow microspheres prepared with PLL1 and PLL2. This material is free of charge via the Internet at http://pubs.acs.org.

JA038953V